

## High Confinement Dissipative Divertor Operation on Alcator C-Mod

J.A. Goetz, B. LaBombard, B. Lipschultz, C.S. Pitcher, J.L. Terry, C. Boswell, S. Gangadhara, D. Pappas, J. Weaver,<sup>a)</sup> B. Welch,<sup>a),b)</sup> R.L. Boivin, P. Bonoli, C. Fiore, R. Granetz, M. Greenwald, A. Hubbard, I. Hutchinson, J. Irby, E. Marmor, D. Mossessian, M. Porkolab, J. Rice, W.L. Rowan,<sup>c)</sup> G. Schilling,<sup>d)</sup> J. Snipes, Y. Takase,<sup>e)</sup> S. Wolfe, and S. Wukitch

*Plasma Science & Fusion Center, Massachusetts Institute of Technology, Cambridge, MA 02139, USA*

Alcator C-Mod [I.H. Hutchinson, *et al.*, Phys. Plasmas **1**, 1511 (1994)] has operated a High-confinement-mode (H-mode) plasma together with a dissipative divertor and low core  $Z_{\text{eff}}$ . The initially attached plasma is characterized by steady-state enhancement factor,  $H_{\text{ITER89P}}$  [P.N. Yushmanov, *et al.*, Nucl. Fusion **30**, 1999 (1990)], of 1.9, central  $Z_{\text{eff}}$  of 1.1, and a radiative fraction of ~50%. Feedback control of a nitrogen gas puff is used to increase radiative losses in both the core/edge and divertor plasmas in almost equal amounts. Simultaneously, the core plasma maintains  $H_{\text{ITER89P}}$  of 1.6 and  $Z_{\text{eff}}$  of 1.4 in this nearly 100% radiative state. The power and particle flux to the divertor plates have been reduced to very low levels while the core plasma is relatively unchanged by the dissipative nature of the divertor.

<sup>a)</sup> Institute for Plasma Research, University of Maryland, College Park, MD 20742

<sup>b)</sup> presently at Applied Research Center, Newport News, VA 23606.

<sup>c)</sup> Fusion Research Center, University of Texas at Austin, Austin, TX 78712

<sup>d)</sup> Princeton Plasma Physics Laboratory, Princeton, NJ 08543

<sup>e)</sup> presently at University of Tokyo, Tokyo, Japan

PACS Numbers: 52.25.Vy, 52.40.Hf, 52.55.Fa

## I. INTRODUCTION

A fusion reactor, e.g. the International Thermonuclear Experimental Reactor (ITER)<sup>1</sup>, will most likely need to operate with a high-confinement (H-mode)<sup>2</sup> plasma that remains clean.<sup>3</sup> The large amount of power flowing in the scrape-off layer (SOL) of such a reactor will need to be reduced to technically feasible levels before it reaches the divertor plates or first wall. Dissipative divertor scenarios, such as the radiative and detached divertor<sup>4,5</sup> offer a solution to the problems of reducing the peak power and erosion of divertor components to acceptable levels.

In current limiter and divertor tokamaks, impurities have been used to achieve detachment in enhanced confinement plasmas.<sup>6-11</sup> These plasmas have high fractional radiated powers, small and frequent Edge Localized Modes (ELMs) and reduced power loads. However, the  $Z_{\text{eff}}$  arising from the puffed impurities is usually too high, typically  $Z_{\text{eff}} > 2$ , and the degradation in energy confinement enhancement factor,  $H_{\text{ITER89P}}$ <sup>12</sup>, too great to maintain a burning plasma in a reactor. The most critical parameters for the ITER operating point are  $H_{\text{ITER89P}} > 1.8$ ,  $Z_{\text{eff}} < 1.6$ , and fractional radiated power of 75%.<sup>3,13</sup>

This paper will report results recently obtained from Alcator C-Mod in which a high-confinement, clean core plasma has been maintained in conjunction with a dissipative divertor. The divertor geometry and the diagnostics used in these studies are described in Section II. Dissipative divertor H-mode operation with nitrogen puffing is discussed in Section III. A discussion of the observed dissipative divertor characteristics is presented in Section IV.

## II. EXPERIMENT DESCRIPTION

Alcator C-Mod<sup>14</sup> is a compact, high field tokamak with a “vertical-plate” divertor geometry. It operates routinely with a dissipative divertor, *i.e.*, large fractions (>50%) of the SOL power are radiated. Parallel heat flux in the scrape-off layer,  $q_{\parallel}^{\text{SOL}} \approx 0.6$

GW m<sup>-2</sup>, approaches that predicted for a fusion reactor (~1 GW m<sup>-2</sup>). The density in the divertor region can be greater than 1 x 10<sup>21</sup> m<sup>-3</sup>, thus enhancing the radiative capabilities of the divertor. The divertor plates and first wall are composed of molybdenum. The vacuum chamber is boronized on a biweekly schedule. The central Z<sub>eff</sub> remains low even with this all metal design.

Experimental data reported here were obtained from 5.7 Tesla, lower single-null deuterium discharges utilizing ion cyclotron range of frequency (ICRF) heating at the second harmonic of deuterium. More specific details of the design, operational capabilities and diagnostics of Alcator C-Mod can be found in Ref. 14. The relevant details of the divertor geometry used for these experiments can be seen in Figure 1. Shown is the magnetic separatrix for a standard “vertical-plate” discharge. Langmuir probes,<sup>15</sup> bolometers,<sup>4</sup> and visible and VUV spectrometers<sup>16,17</sup> are used to measure the characteristics of these dissipative divertor plasmas. In addition “fast thermocouples”<sup>18</sup> are embedded in the outer divertor plate and are used to measure the divertor surface temperature with fast time response. Together with knowledge of the magnetic geometry and modelling, these measurements provide a measure of the parallel heat flux to the plate.

Core radiation measurements are made with an array of tangentially viewing bolometers whose views span from the center of the plasma to the SOL.<sup>19</sup> The central Z<sub>eff</sub> is calculated from continuum radiation measurements made at 536 nm, with a bandpass of 3 nm, combined with density and temperature measurements. The energy confinement time,  $\tau_E$ , is calculated from  $\tau_E = W_p / (P_{tot} - dW_p/dt)$  where P<sub>tot</sub> is the total input power and W<sub>p</sub> is the plasma stored energy. The EFIT magnetics code<sup>20</sup> is used to calculate the plasma stored energy.

A variety of H-modes is obtained in Alcator C-Mod at various currents, fields, and densities. A particular type of H-mode, dubbed Enhanced D H-mode (EDA H-mode), has been identified on Alcator C-Mod.<sup>21,22</sup> EDA H-mode is noteworthy for good

energy confinement ( $\tau_E = 50-70\text{ms}$ ) with an enhancement factor over low-confinement-mode (L-mode) of  $H_{\text{ITER89P}} \sim 2$ . The average  $\tau_E$  for EDA is only 10-15% shorter than that for H-modes with no ELMs (ELM-free). EDA H-modes have several characteristics that are advantageous with respect to other, similar confinement H-modes. Impurity confinement times of 50-150 ms have been measured in EDA H-modes, indicating that there is no impurity accumulation. These times are much shorter than those in ELM-free H-mode.<sup>23</sup> No type I ELMs are observed so there are no transient power loads to the divertor surfaces. In fact, ELM activity of any sort is rarely seen in this EDA H-mode. This H-mode also is steady-state in that it is maintained for many energy confinement times or until the ICRF heating is turned off. The electron density, plasma stored energy, radiated power, *etc.* are all steady state in the H-mode phase. Enhanced confinement modes similar to EDA H-mode have been seen in other tokamaks.<sup>24-26</sup>

### **III. COMBINED DISSIPATIVE DIVERTOR, H-MODE OPERATION**

#### **A. Operating scenario**

Detachment of H-mode plasmas with nitrogen puffing has been achieved previously on Alcator C-Mod.<sup>8</sup> At that time, the nitrogen was puffed through capillary tubes located in the divertor floor tiles. By their nature, these tubes have a low conductance and therefore a slow response time. As a consequence, the nitrogen level was too high after detachment occurred and the radiation in the core plasma increased rapidly leading to degradation and/or termination of the H-mode. For the discharges reported in this paper, the nitrogen injection has been improved by puffing through a piezoelectric valve located in a vertical port within 30 cm of the divertor floor plates (Fig. 1). This valve has a response time of 2 ms and has good conductance to the divertor volume.

An additional improvement in nitrogen puffing is feedback on the injection rate. A

dramatic change in the signal of an edge bolometer chord (tangent to the separatrix)<sup>19</sup> upon detachment is evident when the capillary tubes are being used to puff nitrogen. This change is shown in Fig. 2(a). The gas puff onset time is indicated by the dashed line and the detachment time is shown with the dotted line. At ~1 s (dash-dotted line), the plasma undergoes an H->L-mode transition because of the excess radiation from the puffed nitrogen. This edge bolometer chord signal increase became a signature of detachment for feedback purposes. Feedback on the gas injection rate using the edge bolometer signal as the control parameter is performed by the Alcator C-Mod control computer.<sup>27</sup> The temporal behavior of this edge channel with feedback active is shown in Fig. 2(b). Note that after detachment occurs (denoted by the vertical dotted line), the rate of increase in the edge radiation does not change. Soon after detachment, the feedback results in a steady level of enhanced edge radiation.

It is essential that the plasma be in EDA rather than ELM-free H-mode so that impurities do not accumulate in the core plasma with accompanying H-factor degradation.<sup>22</sup> After the EDA H-mode is established, nitrogen gas is injected to increase the divertor radiated power and reduce the plasma temperature in the divertor thereby optimizing conditions for detachment.

## **B. Plasma characteristics**

A comparison of EDA H-mode plasmas with and without a detached outer divertor is detailed in Figs. 3 and 4. The EDA H-mode plasma (without impurity puffing) is denoted by the dashed lines and the dissipative divertor H-mode plasma (with impurity puffing) by the solid lines in both Figures. The core plasma characteristics are shown in Fig. 3 while the edge/divertor plasma characteristics are shown in Fig. 4. The two plasmas shown were chosen for having nearly identical characteristics before the impurity puffing commenced. The inner divertor remains

attached for all these discharges.

The attached EDA H-mode plasma is described first. The total input power,  $P_{in}$ , which consists of Ohmic power plus ICRF power is shown in Fig. 3(a). The ICRF heating pulse [dotted line, Fig. 3(a)] is turned on at 0.6 s and at 0.61 s the plasma enters the EDA H-mode phase (dash-dotted vertical line). The signature of the H-mode transition is the rapid rise in the line-averaged electron density [Fig. 3(b)] and plasma stored energy [Fig. 3(d)]. The radiation from the main plasma,  $P_{rad}^{main}$ , is shown in Fig 3(c). It is seen that ~25% of the input power is radiated in the main plasma. The EDA character of this H-mode is identified by the steady-state nature of the density, stored energy, and radiated power. The core  $Z_{eff}$  [Fig 3(f)] is 1.0-1.1 in the fully developed H-mode. The energy confinement time is 65 ms, which corresponds to  $H_{ITER89P}$  of 1.9 [Fig. 3(e)]. The impurity confinement time,  $\tau_{imp}$ , is measured by following the temporal behavior of trace impurities injected by the laser blow-off method.<sup>28</sup> For the EDA H-mode plasma shown here,  $\tau_{imp}$  is ~ 70 ms.

It has been observed on many tokamaks that the L->H-mode transition threshold depends on the edge temperature.<sup>29,30</sup> On Alcator C-Mod, this distinct threshold in the edge pedestal temperature,  $T_e^{edge}$  (at the normalized poloidal flux radius of 0.95), is ~150 eV.<sup>31</sup> The H->L-mode transition has the same threshold temperature. After the L->H-mode transition,  $T_e^{edge}$  rises well above the threshold [Fig. 4(a)]. The power flowing across the separatrix into the SOL,  $P_{SOL} = P_{in} - P_{rad}^{main}$ , is shown in Fig. 4(b). Because the measured cross-field e-folding length in the SOL for power is ~1 mm, this 2.5 MW corresponds to a parallel heat flux flowing in the SOL of  $q_{||}^{SOL} \sim 0.55 \text{ GW m}^{-2}$ . The 0.9-1.0 MW of power radiated in the divertor,  $P_{rad}^{div}$  is shown in Fig. 4(c). About 40% of the power flowing into the divertor is radiated before it reaches the target plates. The power that reaches the outer divertor plate,  $P_{plate}^{outer}$ , is shown in Fig. 4(d). After the H-mode is established, there is 0.3 - 0.4 MW flowing to the outer divertor plate. A comparable amount of power reaches the inner divertor plate and does not

change significantly throughout the discharge. The temperature of the plasma measured near the outer divertor strike point is 5-6 eV after the transition into H-mode.

A necessary characteristic of detachment is reduction of divertor plasma pressure compared to “upstream” in the SOL. The electron pressure for these H-mode discharges is shown in Fig. 5. For the reference plasma with no impurity puffing, the electron pressure of 800-1000 Pa is conserved along a flux surface from a location “upstream” in the SOL to the divertor plates [Fig. 5(a)]. The pressure ratio,  $p_{\text{upstream}} / p_{\text{plate}}$ , where  $p_{\text{upstream}}$  is the “upstream” pressure and  $p_{\text{plate}}$  is the pressure at the target plate, is  $\sim 1$ . The dissipative nature of the divertor plasma is then increased by puffing nitrogen gas under feedback control beginning at 0.7 s [see Fig. 3(g)]. The detachment on flux surfaces below the outer divertor “nose” (see Fig. 1) is indicated by an increase in the pressure ratio to  $\sim 50$  [Fig. 5(b)]. When the feedback of the nitrogen gas flow is stable, a pressure ratio of  $\sim 5$  is observed. The feedback [Fig. 3(g)] begins to decrease the flow of nitrogen  $\sim 50$  ms after the detachment begins and as such, the time constant and/or gain of the feedback system could be optimized to allow for better control of this pressure ratio.

There is a slight increase in the Ohmic input power and hence the total input power [Fig. 3(a)] as a result of the nitrogen puffing. After divertor detachment (indicated with a dotted vertical line at 0.83 s), the line-averaged electron density [Fig. 3(b)] rises to  $\sim 5 \times 10^{20} \text{ m}^{-3}$  and becomes steady-state at this new value. This change is most likely due to the decrease in screening that is associated with detachment.<sup>32</sup> This leads to better fueling of the plasma and increased impurity penetration across the separatrix. Through the combination of nitrogen puffing and decreased screening, the radiated power in the main plasma increases to about 2 MW, corresponding to a radiative fraction in the core of 50%. There is no significant difference in the core impurity confinement time measured in attached or detached H-mode plasmas. After detachment, the plasma stored energy falls  $\sim 10\%$  [Fig. 3(d)], the energy confinement

time falls to 55 ms and the corresponding  $H_{ITER89P}$  falls 15% to 1.6 [Fig. 3(e)] and the core  $Z_{eff}$  increases to 1.4 [Fig. 3(f)]. This value of  $Z_{eff}$  is still low, below the maximum allowable for ITER. However, the enhancement factor is not quite high enough to meet the requirements.<sup>3</sup>

The edge pedestal temperature [Fig 4(a)] stays above the H->L threshold and the plasma remains in H-mode. The height of the temperature pedestal is decreased by the nitrogen puffing. Because the height of the pedestal is correlated with the enhancement factor,<sup>22</sup> the drop in  $H_{ITER89P}$  is most likely due to this change in height. Due to the increased main plasma radiation,  $P_{SOL}$  [Fig. 4(b)] falls to ~2 MW which corresponds to a  $q_{||}^{SOL}$  of ~0.45 GW m<sup>-2</sup>. The radiated power in the divertor is increased to ~1.6 MW [Fig. 4(c)]. Thus about 80% of the power flowing into the divertor is radiated. The power reaching the outer divertor plate [Figure 4(d)] is < 0.05 MW which is <5% of  $P_{SOL}$ . Before the nitrogen puffing begins, the parallel heat flux to the outer divertor plates as measured with the “fast thermocouples” is 0.4 GW m<sup>-2</sup>. As nitrogen is puffed into the divertor plasma, the parallel heat flux drops to 0.05 GW m<sup>-2</sup> (resolution limit of the diagnostic).

A requirement for detachment (pressure loss) is that ion-neutral collisions dominate over ionization. Theory has shown that this occurs for  $T_e \leq 5$  eV (see e.g. Ref. 5). The electron temperature at the outer divertor strike point, as measured by Langmuir probes, is reduced to as low as 1.5 eV by the nitrogen puffing.<sup>33</sup> The temperature is below the 5 eV threshold in detached regions along the outer divertor plate below the “nose” [Fig. 1]. The temperature near the inner divertor strike point is still ~10 eV indicating that the inner divertor has remained attached.

Bolometer systems are used to determine the local radiation emissivity and the total power loss (photons plus neutral particles) of the plasma. Tomographic analysis of divertor bolometer array chordal measurements yields the magnitude and distribution of the divertor volumetric loss emissivities. The emissivity contours at 0.68



s of the dissipative divertor plasma depicted in Figs. 3 and 4 are shown in Fig. 6(a). During EDA H-mode operation, the largest emissivity is located near the inner divertor and spread along the outer divertor leg of the separatrix [Fig. 6(a)]. For this plasma, the peak in the emissivity has a value of  $25 \text{ MW m}^{-3}$ . As nitrogen is puffed to create a dissipative divertor, the emissivity pattern changes. At 0.9 s, the peak in the emissivity is near the “nose” of the outer divertor and spread along the outer divertor leg [Fig. 6(b)]. The peak in the emissivity now has a value of  $\sim 50 \text{ MW m}^{-3}$ . The appearance of this peak near the “nose” is well correlated with the decrease in the ion saturation current collected by probes embedded in the divertor plates. Also, the peak in the volumetric emissivity remains outside the last-closed-flux-surface (LCFS). This is in contrast to the behavior in detached Ohmic and L-mode discharges where the peak in emissivity moves inside the LCFS.<sup>4</sup> The higher temperatures that exist near the separatrix and the larger  $q_{\parallel}^{\text{SOL}}$  may be responsible for keeping the peak in radiation in the divertor.<sup>8</sup>

## IV. DISCUSSION

### A. Particle, momentum, and energy loss

Reductions in plasma pressure and heat flux at the divertor plates relative to the plasma midplane are two characteristics of detached plasmas. Detachment also results in low electron temperature and particle flux at the target. Because of the low temperature, volume recombination has been proposed as a possible ion sink to explain this reduction of particle flux upon detachment.<sup>34-36</sup> Measurements of volume recombination in Alcator C-Mod are made by utilizing observations of the Balmer and Lyman series spectra emitted from recombining regions.<sup>16</sup> Up to 75% of the observed ion loss in detached Ohmic plasmas can be accounted for by volume recombination.<sup>17</sup> However, there is little volume recombination observed in these H-mode plasmas [Fig 7(a)]. In fact, after the nitrogen gas is puffed and the outer divertor

detaches, the observed recombination drops. This emphasizes the fact that a strong recombination sink is not necessary to reduce the ion current to the plates in these H-mode plasmas. A primary factor in particle loss in dissipative divertor H-mode plasmas is a decrease in the ion source due to the lowering of the power flowing into the ionization region [Fig 7(a)].<sup>17</sup>

The loss in plasma pressure at the divertor plates predicted by models is the other characteristic of divertor detachment that requires experimental verification. Volume recombination and ion-neutral collisions can transfer momentum from ions to neutrals.<sup>33,34,37</sup> The lack of volume recombination observed in these H-mode plasmas indicates that the loss in pressure upon detachment, in these cases, is not due to this process.

Ion-neutral collisions are effective as a momentum sink only if the velocity differential between the species is significant. Measurements of the velocities of deuterium neutrals and impurity ions have been made<sup>33,38</sup> with a high-resolution spectrometer.<sup>39</sup> In an H-mode plasma, there is a significant difference in the velocities determined from the measured Doppler shifts [Fig. 7(b)]. This difference persists even after nitrogen puffing has caused detachment of the outer divertor. Because of this flow differential, the ions will experience friction against the neutrals as they flow to the plate. The loss of momentum (pressure) is proportional to the difference in flow velocity between the neutrals and ions. A calculation of the pressure loss yields a value of ~1000 Pa which is consistent with the observed electron pressure loss [Figure 5(b)].<sup>33</sup>

Neutral particles can potentially play an important role in removing energy from the divertor plasma. Comparisons of the radiation intensities measured by an extreme-ultraviolet (XUV) spectrograph and bolometers along the same line-of-sight have been made previously in detached Ohmic plasmas.<sup>4</sup> The bolometer measures all the radiation emitted from the plasma plus the power removed from the plasma by

charge-exchange neutrals. In the dissipative divertor regime, the bolometer and XUV radiation time histories were strikingly different, with the bolometer measuring more power. This discrepancy in the temporal behavior of the two measurements points to the role of charge-exchange neutrals as an important loss mechanism in the high density, dissipative divertor.

In order to examine the role of neutrals in the power balance more systematically, a technique for filtering neutral particles from the bolometer line-of-sight has been developed. The bolometer camera housing is filled with deuterium or helium gas to a pressure sufficient to cause small angle scattering of incoming neutrals before they impinge on the bolometer detector. Changes to the sensitivity and cooling of the bolometer must be taken into account when using this “gas filter”. This technique has been applied to the dissipative divertor H-mode plasma shown in Figs. 3 and 4. Helium gas was puffed into the “ledge bolometer” camera (see Fig. 1) to form the “filter” beginning at about 1 s with the “filter” being fully formed by 1.1 s. In Fig 7(c) it is seen that an upper limit of  $\sim 0.1\text{-}0.15$  MW out of  $\sim 1.6$  MW of the power measured by the bolometers are carried by neutral particles. The errors in this technique are large and may account for all of the observed power loss. By examining the time histories of the individual bolometer chords, it is seen that most of the neutral particles detected are on bolometer chords through the x-point and above.

## **B. Impurity transport**

The issues of impurity transport and exhaust are particularly important when dealing with dissipative divertor operation that is realized through impurity puffing. Impurities must be confined to the divertor and SOL with minimal concentrations in the core. This will reduce the detrimental effects on the core such as fuel dilution and cooling, and will enhance the positive effects of the dissipative divertor. Two measures of divertor retention are impurity compression and impurity enrichment.<sup>40,41</sup>

Impurity compression is defined as  $C_z = n_{0,z}^{\text{div}} / n_z^{\text{core}}$  where  $n_{0,z}^{\text{div}}$  is the divertor impurity neutral density and  $n_z^{\text{core}}$  is the core impurity ion density. Maximizing compression can result in more power exhausted through radiation in the divertor if the temperature is optimal. Also, with  $n_{0,z}^{\text{div}}$  constant, maximizing compression leads to less contamination of the core plasma. Impurity enrichment is defined as  $\epsilon_z = C_z / C_D$ , where  $C_D$  is the deuterium compression. Impurity particle exhaust is enhanced by enriching the impurity level with respect to the fuel gas in the divertor.

Measurements of the impurity compression and enrichment have been made for a variety of discharge conditions<sup>42</sup> including H-modes with a detached outer divertor. Argon is normally puffed in trace amounts for central ion temperature and rotation measurements. In an attached EDA H-mode plasma,  $C_{\text{Ar}}$  is  $\sim 50$  and  $\epsilon_{\text{Ar}}$  is  $\sim 5$ . Parallel deuterium ion flows toward the divertor in the SOL are measured<sup>43</sup> and appear to play a role in keeping the compression high. After the outer divertor becomes detached,  $C_{\text{Ar}}$  and  $\epsilon_{\text{Ar}}$  fall a factor of two. The change in compression and enrichment is due mostly to a change in the screening of the impurity from the core plasma.<sup>32</sup> The amount of neutral impurity in the divertor falls only slightly after the divertor detaches. This decrease in compression and enrichment should be considered as a disadvantage of detached divertor operation.<sup>4</sup>

### C. Radiation Effects

Attempts have been made to detach H-mode plasmas using neon and argon as the puffed impurity gas.<sup>8</sup> Unlike nitrogen, these are fully recycling gases. In contrast to the nitrogen injection experiments, these attempts were not successful in producing a detached divertor. Table I lists the change in radiation emissivity measured in the edge of the main plasma and in the divertor plasma that is induced by nitrogen, neon, and argon puffing. It is seen that all gases increase the radiation from the edge plasma which in turn decreases the inferred power flowing into the SOL and divertor.

Little or no increases in divertor radiation were observed when using neon and argon.

To induce detachment, the temperature at the divertor plate must be reduced below  $\sim 5$  eV. For a constant upstream density, this temperature is related to SOL parameters by  $T_e = P_{\text{SOL}}^{10/7} (1 - f_{\text{rad}})^2$ , where  $f_{\text{rad}} = P_{\text{rad}}^{\text{div}} / P_{\text{SOL}}$  is the fraction of the SOL power lost to radiation.<sup>8</sup> It is seen from this relationship that an increase in divertor radiation is more efficient than a decrease in the power flowing into the SOL in reducing the local divertor temperature and thus inducing detachment. This is a possible explanation of why nitrogen gas puffing in Alcator C-Mod, which increases  $P_{\text{rad}}^{\text{div}}$  and decreases  $P_{\text{SOL}}$ , is more effective in inducing detachment than neon and argon, which only decrease  $P_{\text{SOL}}$ .

Core plasma performance is affected by neon and argon puffing. Enhancement factors for H-modes with neon and argon puffing are degraded. In fact, the  $H_{\text{ITER89P}}$  for these attached cases is below that of detached H-modes with nitrogen puffing.<sup>8</sup> Experiments with neon and krypton puffing have been done to determine the effect of these gases on the edge temperature pedestal.<sup>44</sup> The temperature pedestal clearly decreased in height, as well as width, as the core radiation increased and  $H_{\text{ITER89P}}$  decreased correspondingly. Measured radiation emissivity profiles due to these gases are shown in Fig. 8(a). The profile for nitrogen is also shown. It is seen that neon and krypton radiate inboard of the pedestal region (shaded) and that nitrogen radiates farther out. Emissivity profiles obtained from modelling with the MIST impurity transport code<sup>45</sup> support these measurements [Fig. 8(b)]. The radiation location might be another factor in explaining why detached nitrogen puffing discharges have a higher H-factor than attached Ne and Ar puffing discharges.

## V. SUMMARY

Alcator C-Mod has operated a good confinement H-mode plasma together with a dissipative divertor and low core  $Z_{\text{eff}}$ . The initially attached H-mode plasma is

characterized by steady-state energy confinement enhancement factor  $H_{ITER89P}$  of 1.9, central  $Z_{eff}$  of 1.1, power flowing into the scrape-off-layer of 2.5 MW, and total (divertor and core) radiated power fraction of  $\sim 50\%$ . Feedback control of a nitrogen gas puff was then used to increase radiative losses in both the edge and divertor plasmas, while simultaneously maintaining a core plasma with  $H_{ITER89P} \sim 1.6$ ,  $Z_{eff} \sim 1.4$ , and  $P_{SOL} = 2$  MW. The nitrogen puff increases radiation in the divertor and core/edge plasmas by similar amounts, accomplishing a nearly 100% radiative state. The outer divertor detaches although the inner divertor remains attached. Measurements of the heat flux to the divertor plates using fast thermocouples embedded in the outer divertor plates show that the high parallel heat fluxes ( $0.4 \text{ GW m}^{-2}$ ) of the attached state have been lowered to very low levels ( $0.05 \text{ GW m}^{-2}$ ) by this dissipative divertor.

A number of the essential features of the detachment process have been explored. Volume recombination in the divertor, although measurable, is not significant in these dissipative H-mode plasmas. This indicates that the loss in ion current to the plates is a result of other processes, most likely the reduction of the ion source. There is a significant difference in the ion and neutral flow velocities measured in the divertor under detached conditions. The friction from ion-neutral collisions arising from this parallel flow differential is consistent with the observed electron pressure loss along field lines. Neutral power losses in the divertor have been measured. It is seen that 10% of the total divertor radiated power losses are due to the charge-exchange process. Screening, compression, and enrichment of argon are reduced a factor of about two after divertor detachment.

The effect of different impurity gases on detachment and the H-mode pedestal was also investigated. The use of high-Z recycling gases, *e.g.* neon, argon, and krypton, leads to enhanced radiation at the edge of the main plasma but not in the divertor. Nitrogen puffing increases radiation in both regions and results in divertor

detachment. Divertor radiation appears to be more effective than edge plasma radiation in inducing divertor detachment. Use of high-Z gases results in a greater degradation of core confinement than does nitrogen puffing. This is possibly due to the location of the radiation peak, which for the high-Z gases is inboard of the pedestal location.

Divertor detachment in enhanced confinement plasmas has been achieved in many limiter and divertor tokamaks using puffed impurities such as neon and argon.<sup>6,7,9-11</sup> However, either the  $Z_{\text{eff}}$  arising from the puffed impurities is too high or the energy degradation is too great to meet the ITER requirements of  $H_{\text{ITER89P}} > 1.8$  and  $Z_{\text{eff}} < 1.6$ .<sup>3</sup> Encouraging results from Alcator C-Mod have shown that combined dissipative divertor H-mode operation can be achieved with high parallel power flux,  $q_{\text{II}}^{\text{SOL}} \sim 0.5 \text{ GW m}^{-2}$ , good confinement,  $H_{\text{ITER89P}} \sim 1.6$ , and a clean core plasma,  $Z_{\text{eff}} \sim 1.4$ .

The energy enhancement factor achieved in Alcator C-Mod needs to be improved to maintain a burning plasma in ITER.<sup>3</sup> In Alcator C-Mod there is a linear relation between the edge temperature and global confinement.<sup>22</sup> If the edge temperature is enhanced by better wall-conditioning, better tailoring of the impurity puff, using different impurities, or improving the screening of impurities from the core plasma, a better H-factor should result. However, in any scenario, the power flowing to the divertor must be kept at an acceptable level.

## ACKNOWLEDGMENTS

The authors wish to thank the Alcator C-Mod engineering and technical staffs for maintenance and operation of the tokamak. This work is supported by the U.S. Department of Energy Contract # DE-AC02-78ET51013.

## REFERENCES

- <sup>1</sup>N.A. Uckan and the ITER Physics Group (compilers), *ITER Physics Design Guidelines* (International Atomic Energy Agency, Vienna, 1990).
- <sup>2</sup>F. Wagner, G. Becker, K. Behringer, *et al.*, Phys. Rev. Lett. **49**, 1408 (1982).
- <sup>3</sup>G. Janeschitz, H.D. Pacher, G. Federici, *et al.*, in *Proceedings of the 16th International Atomic Energy Agency Fusion Energy Conference* (International Atomic Energy Agency, Vienna, 1997), **Vol II**, 755.
- <sup>4</sup>J.A. Goetz, C. Kurz, B. LaBombard, *et al.*, Phys. Plasmas **3**, 1908 (1996).
- <sup>5</sup>C.S. Pitcher and P.C. Stangeby, Plasma Phys. Control. Fusion, **39**, 779 (1997).
- <sup>6</sup>S.L. Allen, A.S. Bozek, N.H. Brooks, *et al.*, Plasma Phys. Control. Fusion **37**, A191 (1995).
- <sup>7</sup>K. Itami and the JT60 Team, Plasma Phys. Control. Fusion **37**, A255 (1995).
- <sup>8</sup>B. Lipschultz, J.A. Goetz, B. LaBombard, G.M. McCracken, H. Ohkawa, Y. Takase, and J.L. Terry, J. Nucl. Mater. **241-243**, 771 (1997).
- <sup>9</sup>G.F. Matthews for the JET Team, Plasma Phys. Control. Fusion **37**, A227 (1995).
- <sup>10</sup>J. Neuhauser, M. Alexander, G. Becker, *et al.*, Plasma Phys. Control. Fusion **37**, A37 (1995).
- <sup>11</sup>U. Samm, G. Bertschinger, P. Bogen, *et al.*, Plasma Phys. Control. Fusion **35**, B167 (1993).
- <sup>12</sup>P.N. Yushmanov, T. Takizuka, K.S. Riedel, O.J.W.F. Kardaun, J.G. Cordey, S.M. Kaye, and D.E. Post, Nucl. Fusion **30**, 1999 (1990)
- <sup>13</sup>S. Putvinski, R. Aymar, D. Boucher, *et al.*, in *Proceedings of the 16th International Atomic Energy Agency Fusion Energy Conference* (International Atomic Energy Agency, Vienna, 1997), **Vol II**, 737.
- <sup>14</sup>I.H. Hutchinson, R. Boivin, F. Bombarda, *et al.*, Phys. Plasmas **1**, 1511 (1994).
- <sup>15</sup>B. LaBombard, J. Goetz, C. Kurz, *et al.*, Phys. Plasmas **2**, 2242 (1995).
- <sup>16</sup>J.L. Terry, B. Lipschultz, A. Yu Pigarov, *et al.*, Phys. Plasmas **5**, 1759 (1998).



- <sup>17</sup>B. Lipschultz, J.L. Terry, C. Boswell, *et al.*, "The role of particle sinks and sources in Alcator C-Mod detached divertor discharges", submitted to *Phys. Plasmas* (1998)
- <sup>18</sup>S. Gangadhara, B. LaBombard, B. Lipschultz, and N. Pierce, *Bull. Am. Phys. Soc.* **41**, 1550 (1996).
- <sup>19</sup>J.A. Goetz, B. Lipschultz, M.A. Graf, C. Kurz, R. Nachtrieb, J.A. Snipes, and J.L. Terry, *J. Nucl. Mater.* **220-222**, 971 (1995).
- <sup>20</sup>L.L. Lao, H. St. John, R.D. Stambaugh, A.G. Kellman, and W. Pfeiffer, *Nucl. Fusion* **25**, 1611 (1985).
- <sup>21</sup>Y. Takase, R.L. Boivin, F. Bombarda, *et al.*, *Phys. Plasmas* **4**, 1647 (1997)
- <sup>22</sup>M. Greenwald, R.L. Boivin, F. Bombarda, *et al.*, *Nucl. Fusion* **37**, 793 (1997)
- <sup>23</sup>M. Greenwald, J. Rice, R. Boivin, *et al.*, "Transport in Alcator C-Mod H-Modes", submitted to *Phys. Plasmas*, 1998.
- <sup>24</sup>M. Bures, D.J. Campbell, N.A.C. Gottardi, *et al.*, *Nuclear Fusion* **32**, 539 (1992).
- <sup>25</sup>T. Ozeki, M.S. Chu, L.L. Lao, T.S. Taylor, M.S. Chance, S. Kinoshita, K.H. Burrell, and R.D. Stambaugh, *Nucl. Fusion* **30**, 1425 (1990).
- <sup>26</sup>Y. Kamada, R. Yoshino, Y. Neyatani, *et al.*, *Plasma Phys. Control. Fusion* **38**, 1387 (1996).
- <sup>27</sup>S. Horne, M. Greenwald, I. Hutchinson, S. Wolfe, G. Tinios, T. Fredian, and J. Stillerman, in *Proceedings of the 15th IEEE/NPSS Symposium, Fusion Engineering* (Institute of Electrical and Electronics Engineers, Piscataway, NJ, 1994), **Vol. 1**, 242.
- <sup>28</sup>E.S. Marmor, J. Cecchi, and S. Cohen, *Rev. Sci. Instrum.* **46**, 1149 (1975).
- <sup>29</sup>F. Wagner, M. Keilhacker, G. Becker, *et al.*, *J. Nucl. Mater.* **121**, 103 (1984).
- <sup>30</sup>J.A. Snipes, in *Proceedings of the 24th EPS Conference on Controlled Fusion and Plasma Physics* (European Physical Society, Petit-Lancy, 1997), **Vol. 21A**, 961.
- <sup>31</sup>A.E. Hubbard, R.L. Boivin, J.F. Drake, M. Greenwald, Y. In, J.H. Irby, B.N. Rogers, and J.A. Snipes, *Plasma Phys. Control. Fusion* **40**, 689 (1998).
- <sup>32</sup>G.M. McCracken, B. Lipschultz, B. LaBombard, *et al.*, *Phys. Plasmas* **4**, 1681 (1997).

- <sup>33</sup>C.S. Pitcher, J.A. Goetz, B. LaBombard, B. Lipschultz, J.L. Weaver, and B.L. Welch, "The Role of Friction in SOL Pressure Balance in Alcator C-Mod", accepted to J. Nucl. Mater. (1998).
- <sup>34</sup>S.I. Krasheninnikov, A. Yu. Pigarov, D.A. Knoll, *et al.*, Phys. Plasmas **4**, 1638 (1997).
- <sup>35</sup>A. Loarte, J. Nucl. Mater. **241-243**, 118 (1997).
- <sup>36</sup>K. Borrass, D. Coster, D. Reiter, and R. Schneider, J. Nucl. Mater. **241-243**, 250 (1997).
- <sup>37</sup>P.C. Stangeby, Nucl. Fusion **33**, 1695 (1993).
- <sup>38</sup>B. Lipschultz, C. Boswell, J.A. Goetz, *et al.*, "Detached Divertor Plasmas in Alcator C-Mod: A Study of the Role of Atomic Physics", submitted to the *Proceedings of the 17th International Atomic Energy Agency Fusion Energy Conference*, (1998).
- <sup>39</sup>J.L. Weaver, B. L. Welch, H. R. Griem, *et al.*, "Localization of Emission through Interpretation of Observed Zeeman Pattern", submitted to Rev. Sci. Instrum., 1998.
- <sup>40</sup>M. Shimada, M. Nagami, S. Izumi, *et al.*, Phys. Rev. Lett. **47**, 796 (1981).
- <sup>41</sup>H.S. Bosch, D. Coster, R. Dux, *et al.*, Plasma Phys. Control. Fusion **39**, 1771 (1997).
- <sup>42</sup>J.A. Goetz, B. Lipschultz, C.S. Pitcher, J.L. Terry, P.T. Bonoli, J.E. Rice, and S.J. Wukitch, "Impurity compression and enrichment studies on Alcator C-Mod", accepted to J. Nucl. Mater. (1998).
- <sup>43</sup>B. LaBombard, J.A. Goetz, I.H. Hutchinson, *et al.*, in *Proceedings of the 16th International Atomic Energy Agency Fusion Energy Conference* (International Atomic Energy Agency, Vienna, 1997), **Vol 1**, 825.
- <sup>44</sup>A.E. Hubbard, R.L. Boivin, J.A. Goetz, M. Greenwald, and B. Lipschultz, Bull. Am. Phys. Soc. **43**, 1706 (1998).
- <sup>45</sup>R.A. Hulse, Nucl. Technol./Fusion **3**, 259 (1983).

**TABLE I**

Change in volumetric emissivity for H-mode plasmas with impurity puffing

impurity gas	emissivity change in edge of main plasma	emissivity change in divertor plasma
nitrogen	$\sim 1 \text{ MW m}^{-3}$	$\sim 10 \text{ MW m}^{-3}$
neon	$\sim 1 \text{ MW m}^{-3}$	$0\text{-}2 \text{ MW m}^{-3}$
argon	$\sim 1 \text{ MW m}^{-3}$	$0\text{-}2 \text{ MW m}^{-3}$

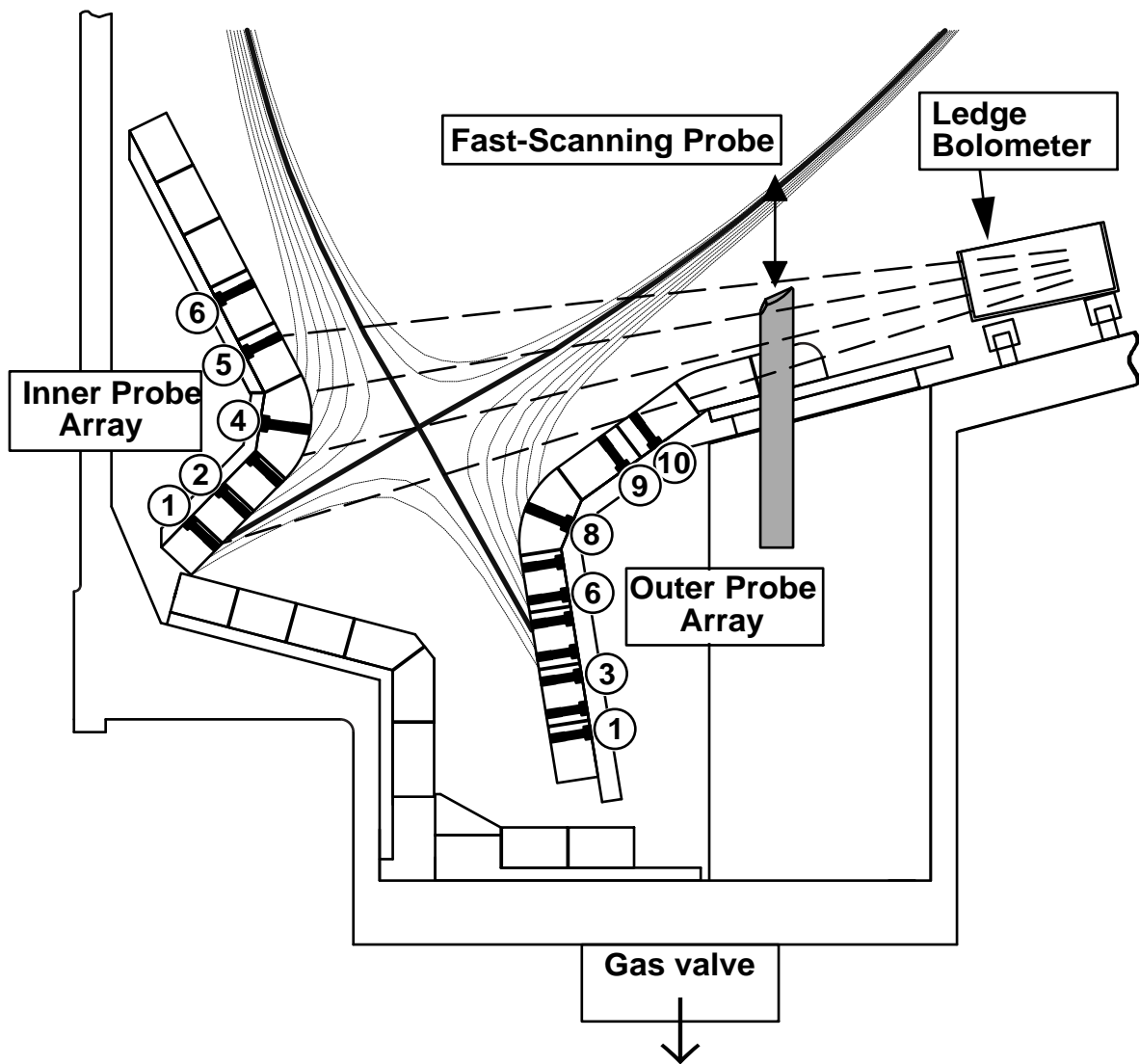


Figure 1. Schematic of the Alcator C-Mod divertor showing the Langmuir probes, the centerline of the views of the “ledge bolometers” and the location of the gas puff valve used in this work. Also shown is the magnetic geometry used for these experiments. The plasma detaches at the outer divertor in regions below the “nose” (outer probe 8).

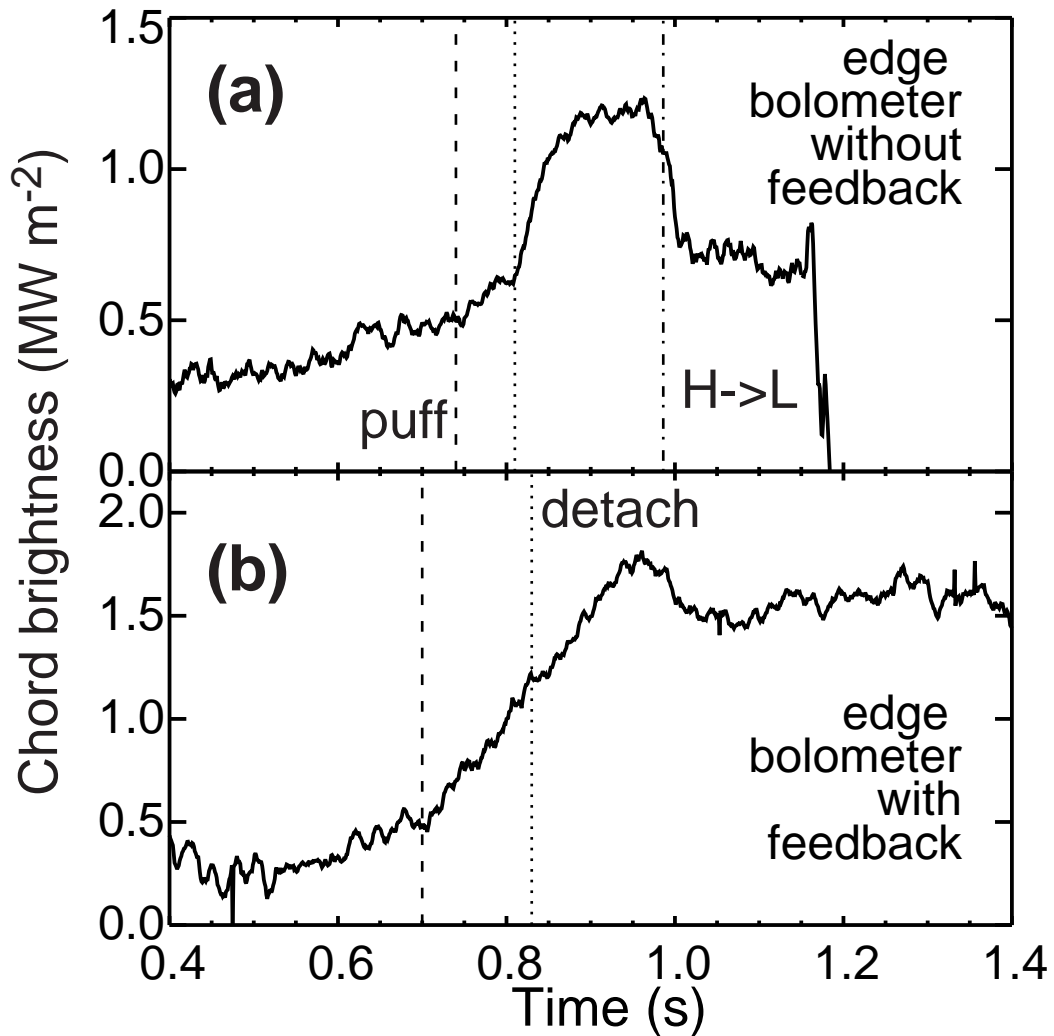


Figure 2. Comparison of the bolometer channel viewing the edge of the main plasma for EDA H-mode discharges without (a) and with (b) feedback on a nitrogen gas puff. The puff start time is indicated with a dashed line and the outer divertor detachment start time is indicated with a dotted line in both (a) and (b). The plasma undergoes an H->L-mode transition at ~1 s in case (a) as indicated by the dash-dotted line. [(a): Shot 960227019; (b): Shot 980213015].

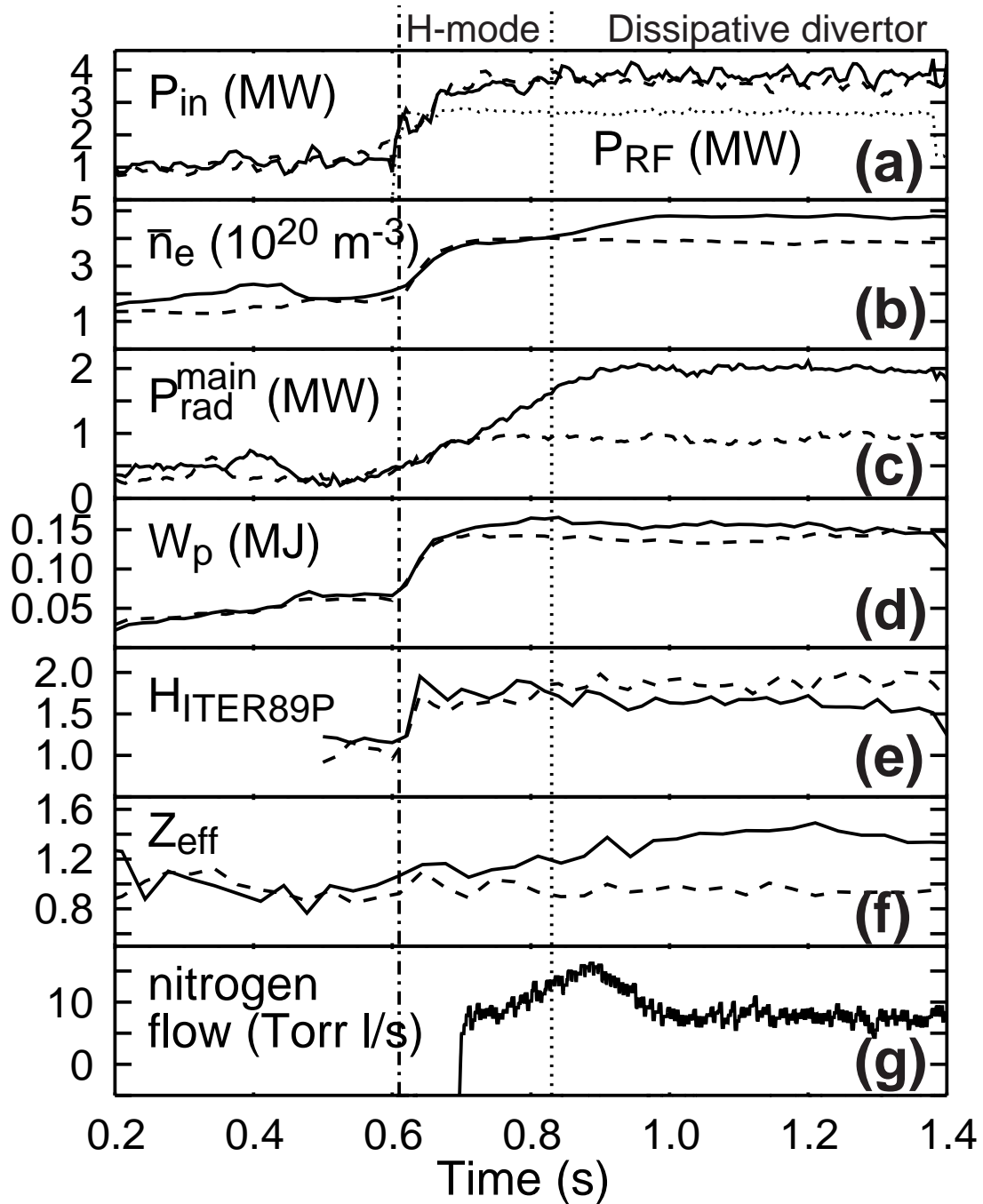


Figure 3. Typical core plasma conditions are shown for an EDA H-mode plasma without nitrogen puffing (dashed lines) and a dissipative divertor H-mode plasma with nitrogen puffing (solid lines). The H-mode transition (for both plasmas) occurs at 0.61s (vertical dash-dotted line), the gas puff begins at 0.7 s, and the outer divertor begins to detach at 0.83 s. (vertical dotted line). The injected ICRF power is shown with the dotted line in (a) and is nearly the same for both plasmas.

[dashed lines: Shot 980213007; solid lines: Shot 980213015].

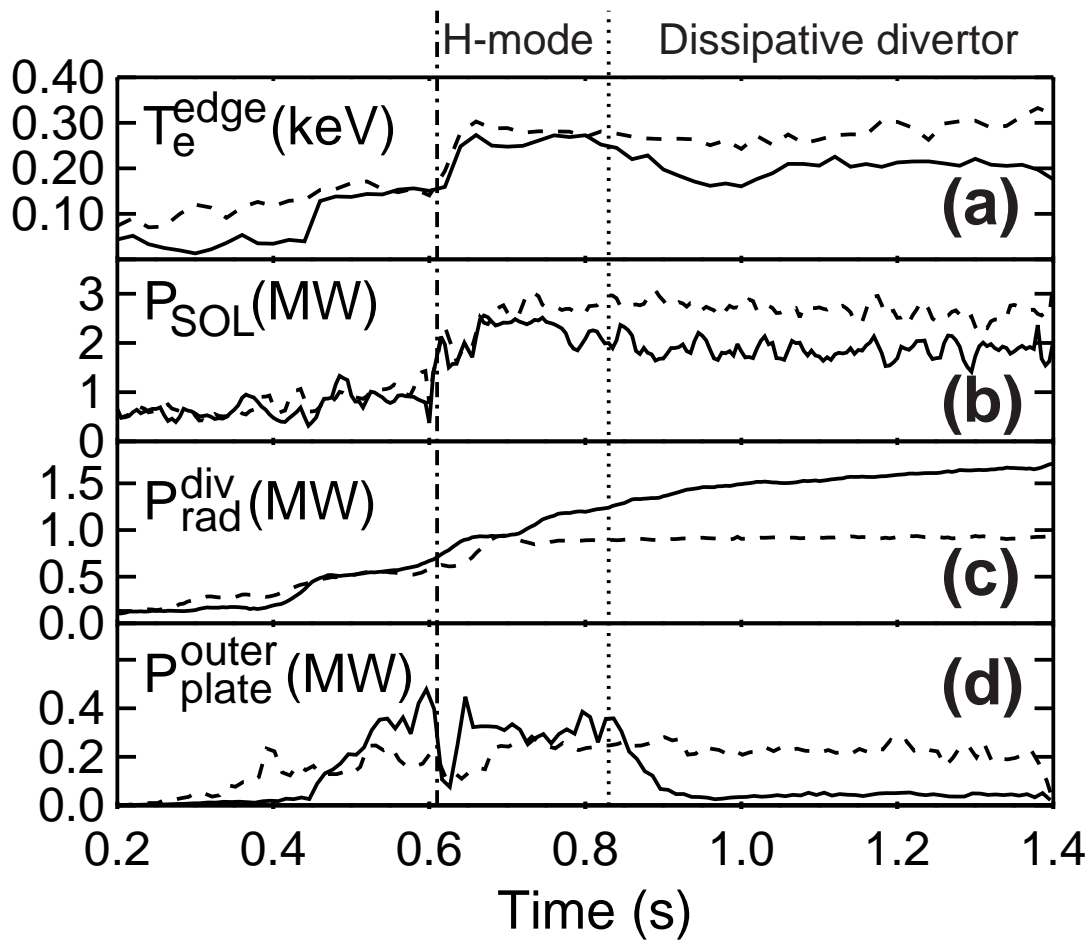


Figure 4. Typical divertor plasma conditions are shown for the discharges of Fig. 3.

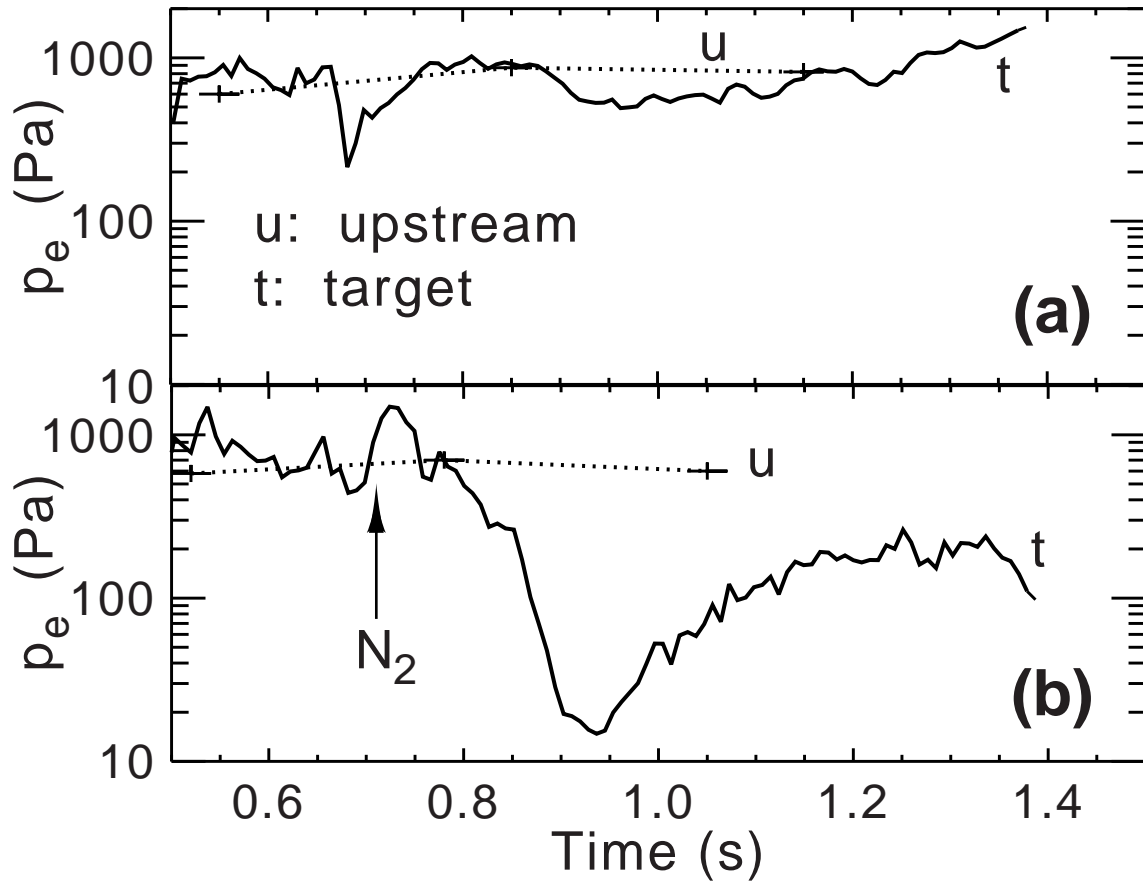


Figure 5. Plasma electron pressure is measured at the target plates (t) with embedded Langmuir probes and “upstream” in the SOL outside of the divertor (u) with a reciprocating Langmuir probe.<sup>15</sup> Pressure is conserved in the EDA H-mode plasma with no impurity puffing (a) but is lost from upstream to the target plate in the dissipative divertor plasma with impurity puffing (b). [(a): Shots 980213019 & 20; (b): Shots 980213014 & 16].



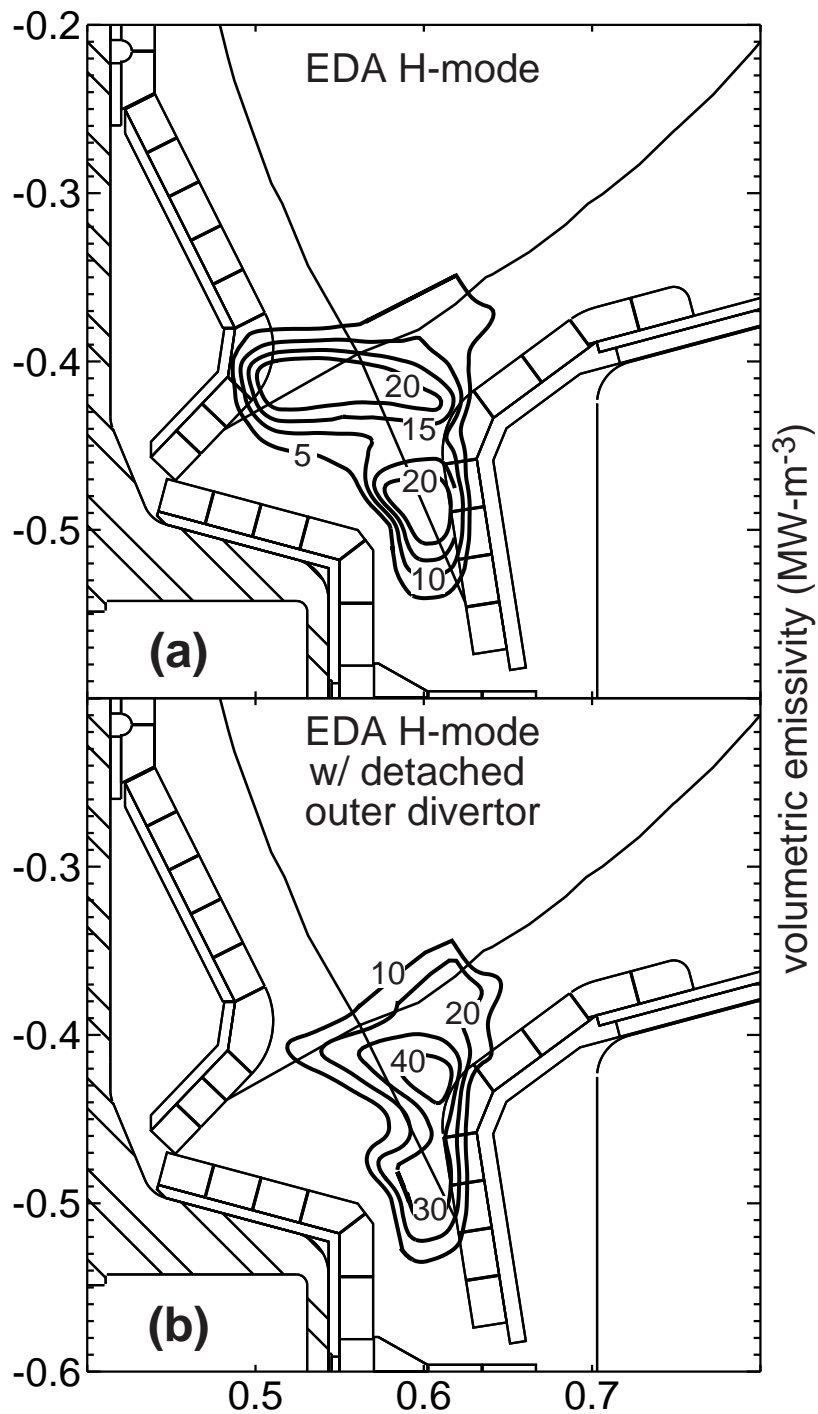


Figure 6. The volumetric emissivity in the divertor region is obtained from bolometer measurements. The emissivity contours from (a) before ( $t = 0.68$  s) and (b) after ( $t = 0.9$  s) the nitrogen puff are shown for the dissipative divertor H-mode depicted in Figs. 3 and 4.

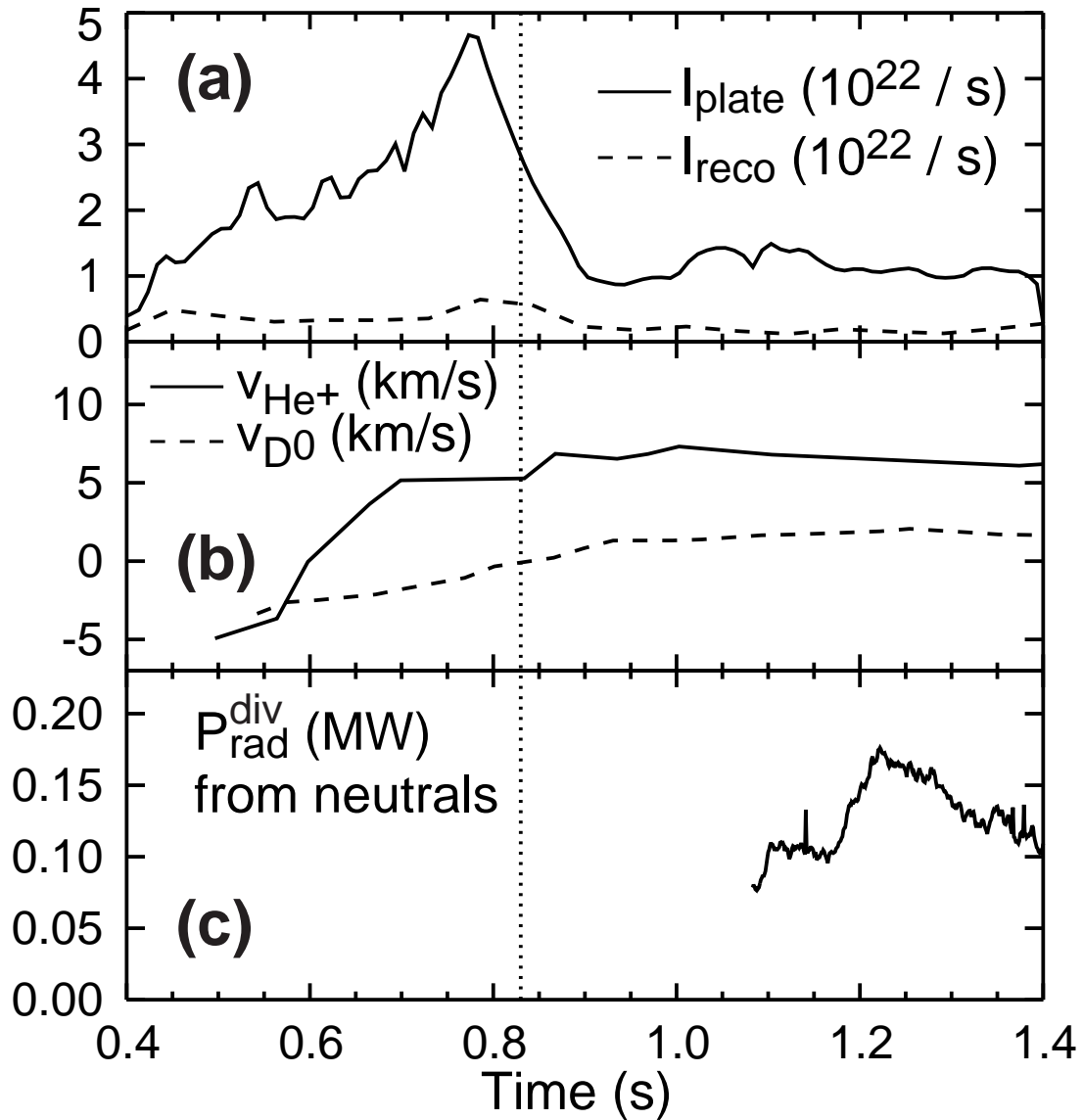


Figure 7. Particle (a), momentum (b), and energy (c) sinks are measured in the divertor for a typical dissipative divertor H-mode plasma. The outer divertor detachment time is shown with the dotted line. The ion saturation current collected by Langmuir probes,  $I_{\text{plate}}$  (solid line), and the measured divertor volume recombination,  $I_{\text{reco}}$  (dashed line), indicate that the ion source,  $I_{\text{source}} = I_{\text{plate}} + I_{\text{reco}}$ , is reduced after detachment (a). The friction arising from the observed ion-neutral flow differential (b) can account for the pressure loss of detachment (Fig. 5). The component of power ascribed to neutral particles (c) in the divertor is measured with bolometers and a “neutral particle filter”. This measurement is performed only after 1.1 s.

[(a): Shot 980213021; (b): Shots 980213014-16; (c): Shot 980213021].

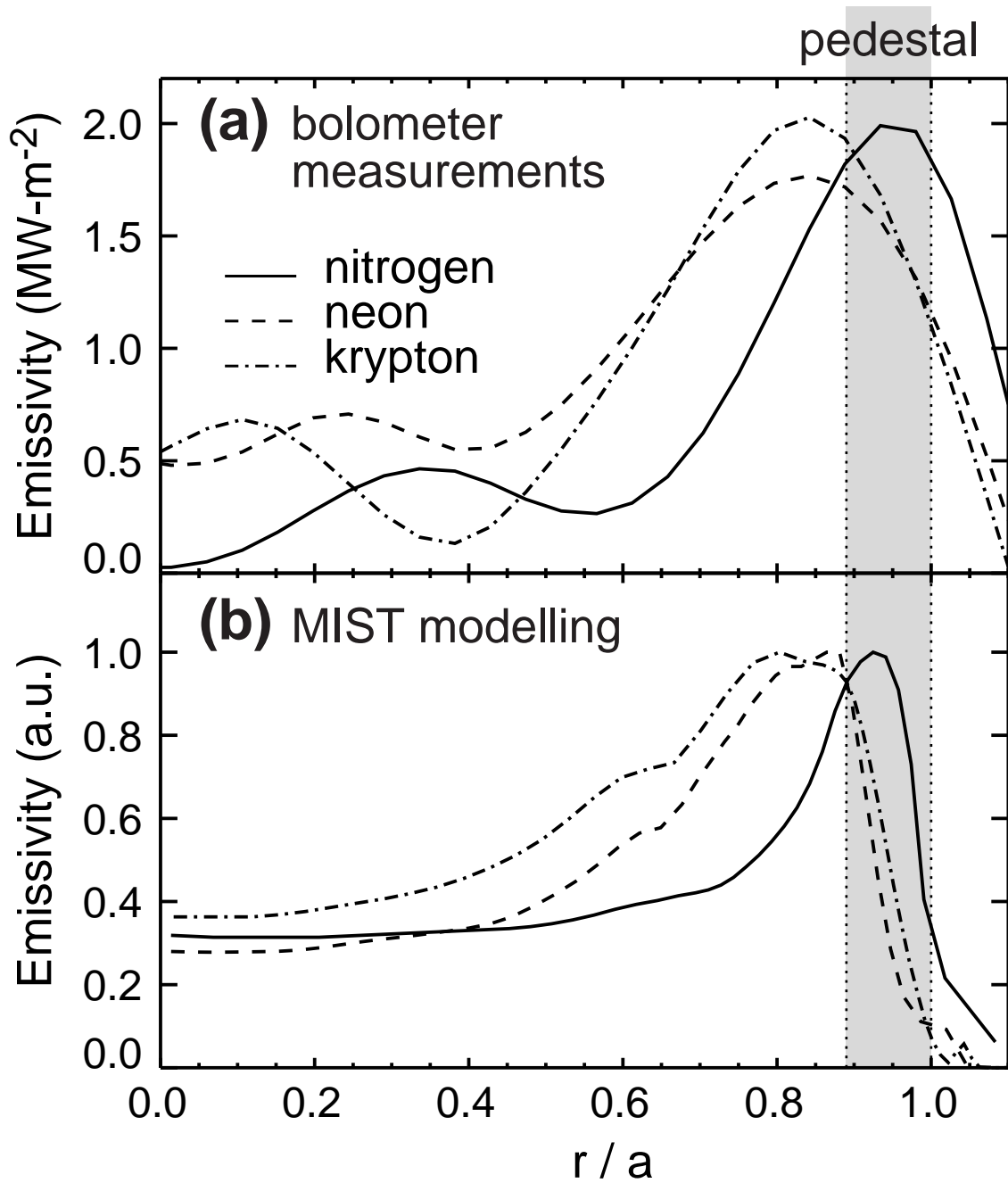


Figure 8. Radiation emissivity profiles are measured (a) and calculated with the MIST impurity transport code (b) for impurities puffed into an EDA H-mode plasma. The pedestal region is shown with the shading.